

Modelling and Optimisation of Up-and Down-Milling Processes for a Representative Pocket Feature

Mariana Dotcheva¹, Krassimir Dotchev^{1#}, and Ivan Popov¹

¹ School of Engineering, University of Portsmouth, Anglesea Building, Anglesea Road, Portsmouth PO1 3DJ England, United Kingdom
Corresponding Author / E-mail: Krassimir.Dotchev@port.ac.uk, TEL: +44-23-9284-2345, FAX: +44-23-9284-2525

KEYWORDS: End-Milling, Surface Profile Error, Finishing Process

This paper presents the specifics of the two types of end-milling, up- and down-milling, in the context of process planning of a finishing operation for machining complex pocket features. An optimisation mechanism is used for a pocket type of end-milling operation with the aim of comparing the results from up- and down-milling. Two sets of cutting conditions have been generated and analysed for each type of end-milling- one with constant parameters for the entire tool path, derived from the worst case of cutting (representing the usual process planning approach) and another set representing the optimised process. The predicted results were verified through experiments. The optimized cutting parameters, when machining the critical corner, demonstrate the important changes in magnitude and direction of the radial cutting-tool deviation and surface error.

Manuscript received: September 11, 2012 / Accepted: February 25, 2013

1. Introduction

Despite tremendous developments in CAM software, cutting-tool technology and machine-tool technology, end-milling results still depend to a large extent on the knowledge inherent within manufacturing staff.¹⁻³ End-milling machining is a complex process in terms of process planning due to intricate geometry, the evolution of new materials, and high-precision requirements of the final product. Consequently, the full potential of the machine tool system is under utilised in many cases. CAD/CAM systems can generate CNC programs based on the part geometry, but they do not help programmers to choose appropriate cutting conditions and other process parameters, such as step over, cutting direction, cutter entrance and exit, and type of transition between the strokes of the tool path. The other issue in finishing pocket milling is determining which type of end-milling should be used: Up-Milling (UM) or Down-Milling (DM). Traditional workshop practice recommends DM for finishing profiling. Some researchers also consider DM as a better method for finishing. Landon *et al.*⁴ state that in the engineering industry, finishing milling using DM aims to preserve the cutting tools and obtain a better surface finish than can be achieved with UM. Hatna *et al.*⁵ recommend DM, because it gives a better load on the cutting edge and allows the use of higher speeds and feed rates. However the research of Lee and Ko⁶ claims that the accuracy of a surface cut by UM is much better than the accuracy of

the same surface machined by DM. This paper investigates further how the type of milling affects the process efficiency and process accuracy. It presents the specifics of UM and DM in the context of optimisation of an end-milling machining process of a pocket-type part feature. The key parameters used for accessing the efficiency and accuracy of the milling processes are Surface Error (SE), radial cutting-tool deviation, surface roughness and the machining time. A comparison of two end-milling operations is presented when UM and DM are applied.

2. Cutting force, tool, and machined surface models

Cutting force model. The specifics of the chip-thickness creation process in UM and DM reflect the direction and the magnitude of the cutting forces (Fig. 1). A mechanistic force model has been adopted as the most appropriate for cutting force analysis in this study. This model⁷ directly represents the effect of the variation of the chip thickness on the cutting forces, and then on the part accuracy. The F_Y cutting force causes the radial cutter deviation in the milling process. In DM it is generally larger than the equivalent force in UM. Although in both cases F_Y direction is the same, in UM the F_Y is towards the machined surface and could cause overcut. In DM, the F_Y force is directed away from the machined surface and could create undercut.

The total instantaneous F_X , F_Y and F_Z force components at the cutter

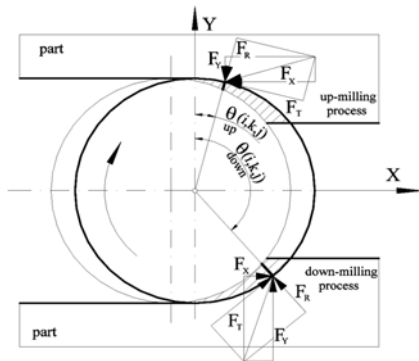


Fig. 1 The cutting forces in up-milling and in down-milling

rotation angle $\theta(i,k,j)$ are the sum of the forces acting on the simultaneously engaged flutes (k) and disk elements (j) in cutting:

$$\begin{cases} F_x(\theta) \\ F_y(\theta) \\ F_z(\theta) \end{cases} = \sum_{k=1}^{N_f} \sum_{j=1}^{N_z} \xi_F(\theta(i, k, j)) \begin{cases} F_x(i, k, j) \\ F_y(i, k, j) \\ F_z(i, k, j) \end{cases} \quad (1)$$

where

$\xi_F(\theta(i, k, j))$ is an index to indicate that tooth at elemental angle rotation i is in the cut at angular position $\theta(i, k, j)$:

$$\xi_F = 1 \text{ if } \tau_{\text{entry angle}} < \theta(i, k, j) < \tau_{\text{exit angle}} \xi_F = 0 - \text{otherwise.}$$

Knowledge of the specifics of the two milling types included in this modelling helps in making effective decisions during the process planning. The proposed mechanistic cutting-force model is a major element of the simulation and the optimisation processes of the end-milling operation. All computer programmes developed for this end-milling simulation have been coded and run using MATLAB.

Cutting tool deflection estimation. To assess the accuracy of the planned milling operations a static model of the deflected cutting tool has been employed which considers the end mill as a cantilever.⁷ The cutting tool is simplified as a two-step cylindrical cantilever beam, due to the distinct geometry of the cutter and the dual-mode deflection of a cutting tool is based on models addressed by Gere and Timoshenko⁸ and Xu et al.⁹

Generation of the machined surface. During the cutting process the surface topography is created by the coordinated movements between the cutting tool and the work-piece. When a helical cutting tool is employed in an end-milling operation several elemental axial disks take part in cutting. Only one of them generates the machined surface topography at a certain moment. The elemental disk that forms the machined surface is the disk $a(j)$ that crosses the surface formation line at a certain rotational angle $\theta(i, k, j)$, as shown in Fig. 2. Although only the deviation of the cutting tool at the crossing point between the helical cutting edge and the surface formation line defines the SE, the other elemental disks that are simultaneously engaged also contribute to the error. In this surface generation mechanism the specifics of the chip formation and cutting forces magnitude and direction in up- and DM play a significant role. The results of the predicted cutter deviation in UM are presented in Fig. 3.

This is an example of finishing end-milling operation when the

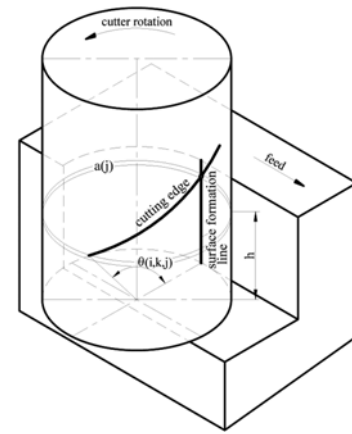


Fig. 2 The process of surface generation in end-milling operation

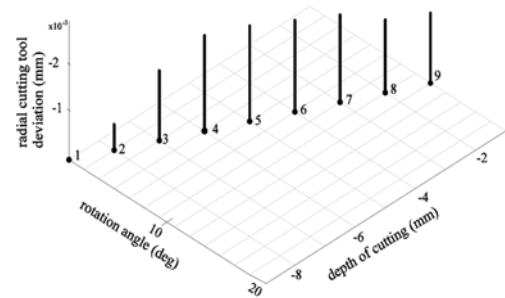


Fig. 3 Cutting tool deflection in up-milling

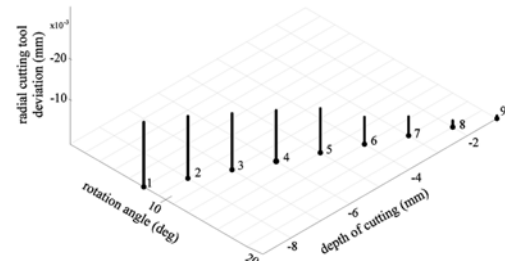


Fig. 4 Cutting tool deflection in down-milling

radial depth of cutting is 0.5 mm and the axial depth of cutting is 9 mm. The adopted model for calculating the cutter deflection allows estimation of the cutting deflection at a given distance as a result of all simultaneous cutting forces.

At the start of cutting during one cutter rotation, when the chip thickness is small and one or two elemental disks are engaged, the deflection is insignificant. In the finishing UM case the largest cutter deflection occurs at the mid-section of the axial depth of cutting, because the number of the engaged elemental disks is greater than the number when disks one and two are crossing the formation line.

The same finishing cutting conditions were applied to DM. The chip thickness is at its largest value at the beginning of cutting for a given elemental disk, and consequently the instantaneous $F_y(i, k, j)$ cutting force has the largest magnitude. The resultant cutting tool deflection for DM process is shown in Fig. 4. At the crossing points 1-5 the cutter deflection is larger compared with points 6-9, when the number of the engaged disks is reducing gradually. Hence, the $F_y(i, k, j)$ cutting forces values reduce due to the points being closer to the clamped end of the cutter. The real trajectory of the cutting tooth is trochoidal. UM and

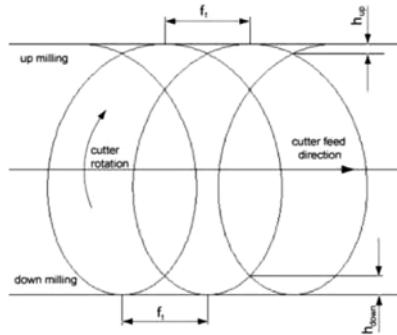


Fig. 5 Trochoidal tool path in up- and down-milling

DM do not use the same part of the trochoidal tooth path during the cutting because of the different rotational directions of the cutter, as shown in Fig. 5. In DM, the height of the feeding marks h_{down} is larger than those in UM h_{up} obtained with the same feed rate. Therefore the surface roughness in DM is expected to be larger compared to UM.

3. The optimisation process for end-milling

The optimisation process used in this section is based on models in section 2 and on 'in tolerance' optimisation strategy developed for finishing end-milling operations.⁷ The strategy adopts a model-based method¹⁰ for optimisation and is an off-line technique that adjusts the controlled parameter to the maximum allowed limit, before the actual cutting, based on the predicted data from the process model. The feed rate is the controlled parameter in the optimisation process and the required surface tolerance and the surface roughness are the constraints. For the general case, it is assumed that the cutting tool, machine tool and machining process are determined, and the dimensional accuracy and surface roughness are specified. As the cutting-tool deviation reflects the action of the cutting forces and is the dominant parameter in the machining error estimation, it takes the major role in the optimisation process. The optimised end-milling processes are judged in terms of a combination of surface accuracy, surface roughness and machining (finishing) time. The radial component of the cutter deflection contributes to the surface accuracy and its magnitude is controlled in certain limits defined from the required surface tolerance. The maximum allowable value for the radial cutter deflection when the worst cutting conditions for a given tool path are applied, is called the limiting radial deviation δ_{lim} . The limiting radial deviation defines the maximum cutting force (F_{max}) and the required feed rate for achieving the surface accuracy. The limiting radial deviation of the cutting-tool is derived by taking into account the required surface tolerance ($\pm\Delta_{total}$), the machine tool geometric errors (Δ_{mt}), the tolerance of generating the tool path (Δ_{tp}), the tolerance of the diameter of the cutting-tool (Δ_{ct}), and the additional cutting process errors (Δ_{add}). The key relation between these parameters is given below:

$$\Delta_{total} = |\delta_{lim}| + |\Delta_{tp}| + |\Delta_{ct}| + |\Delta_{mt}| + |\Delta_{add}| \quad (2)$$

The new optimised feed rate (f_{opt}) is then obtained using the limiting radial cutting-tool deviation (δ_{lim}), the maximum radial deviation produced by constant feed rate ($\delta_{rad}(f_{con})$) at every important tool

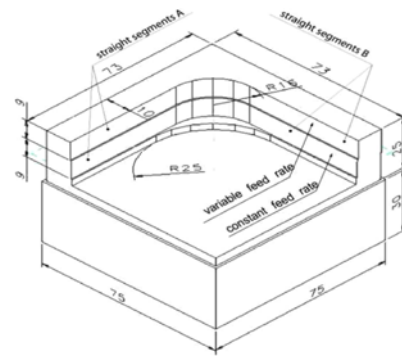


Fig. 6 The geometry of the test piece surfaces and coordinates of the key points of the corner

Table 1 The experimental data for the cutting processes.

Cutting tool:	16 mm HSS 3 fluted with 30° helix angle
Cutting tool rake angle:	7°
Cutter overall length:	77 mm
Cutter effective length:	50 mm
Flute length:	30 mm
Cutting-tool material:	High Speed Steel (HSS)
Modulus of elasticity:	200 GN/m ² for HSS (Ashby and Jones 1996)
Test-piece material:	Aluminium alloy 6082
Cutting-force coefficients:	$K_T = 1292(t_c)^{-0.1657}$ $K_R = 0.4477(t_c)^{-0.01307}$
Machine tool:	Mikron HSM 400
CMM:	Mitutoyo Euro-C Apex 121210

location (X_c, Y_c), and the constant feed rate (f_{con}):

$$f_{opt}(X_c, Y_c) = f_{con} \frac{\delta_{lim}}{\delta_{rad}(f_{con})} \quad (3)$$

The optimisation process has been applied to a pocket-type test piece presented in Fig. 6, and the inside corner geometry is highlighted.

The roughing radius was set at 25 mm and the finished inside-corner radius at 16 mm. The difference between the radius of the roughing cutter and the radius of the finished corner creates a cutting geometry with variable chip thickness representing the general case of corner milling. The test piece incorporates two identical surfaces, which allows a paired-comparison experiment to be implemented. The two controlled surfaces of a test piece were cut with two different cutting conditions. The first was derived from the worst-case of cutting and the second one was obtained after applying the optimisation strategy to the same contour with variable geometry. The required overall tolerance for the given contour was set at $\Delta_{total} = \pm 0.05$ mm. The tool path generating tolerance was $\Delta_{tp} = \pm 0.005$ mm, the cutting-tool tolerance was $\Delta_{ct} = \pm 0.005$ mm, and the additional cutting process error was $\Delta_{add} = \pm 0.005$ mm. The geometric accuracy of the machine tool (Mikron HSM 400) used in the experiments was specified at $\Delta_{mt} = \pm 0.005$ mm. Taking into consideration the above tolerances, the allowable deviation of the cutting tool under the cutting forces was calculated to be $\delta_{lim} = \pm 0.03$ mm. This accuracy constrain was applied to both types of end-milling: up- and DM. The cutting tool and work-piece data used in the experimental work is presented in Table 1 as K_R and K_T are radial and tangential cutting force coefficients.

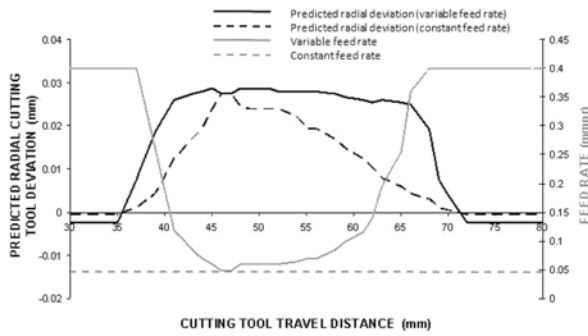


Fig. 7 Constant and variable cutting conditions in up-milling

Up-milling modelling and optimization. The optimization produced two sets of results. The first set presents the constant cutting condition when the entire tool path is cut with the same feed rate and the second set of data presents the optimised variable cutting conditions. It is a result from the application of the adjustment mechanism to the whole tool path, while satisfying the accuracy requirements. After the constant and variable feed rate cutting conditions have been generated the corresponding predicted radial cutter deviation based on the cutting forces have been synthesised and compared. Fig. 7 shows the results from the optimisation process when UM is used.

The two contrasting feed rates are shown together, with respect to cutting-tool travel distance. The constant feed rate was defined at 0.048 mmpr. The optimised feed-rate varies along the tool path starting with the maximum allowable value for the straight cutting when the chip thickness is constant and the load is low. Then it decelerates to the constant feed-rate value at the point of peak chip thickness (i.e. the start of the corner), and then accelerates back to a maximum according to the chip load at every cutter position. The feed rate in the straight segment is lower than the maximum allowable from the cutting-tool deviation condition because of the limitation of the surface roughness criterion, which was set by the arithmetical mean deviation of the profile to be $R_a = 0.8 \mu\text{m}$. The transient cutting conditions prior to the point of maximum chip thickness reduces the feed rate before the corner, which limits tool loading and creates an overall smoother milling process. At the end of the corner, the chip thickness becomes constant and equal to the chip thickness at the straight part of the pocket, and the feed rate obtains the highest allowable rate. The positive direction of the predicted cutter deflection means that the deviation is toward the machined surface, and the negative deviation is directed out of the nominal part surface. In UM when the engagement angle is small the deviation is negative, but at the corner and in the transient sections of the tool path when the engagement angle is changeable and larger, the predicted cutter deviation is directed towards the machined surface.

Down-milling modelling and optimisation. The same optimisation requirements were applied when DM was assessed. The results from the optimisation process and from the constant cutting condition are shown in Fig. 8. For the case of DM the predicted cutter radial deviation is entirely negative. The expected SE component, which is as a result of the radial deviation of the cutting tool, is directed out of the machined surface. If the milling operation is not well planned, this could lead to surface undercut. If the machined surface is out of tolerance as a result of DM undercut it could be reworked, and the

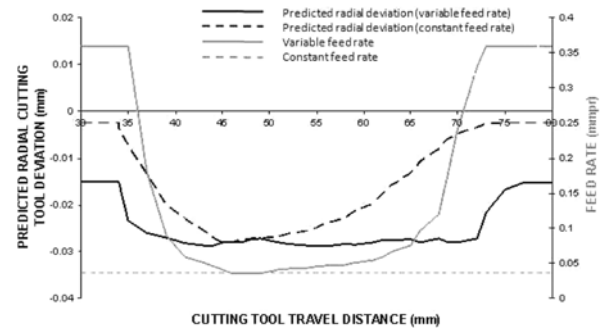


Fig. 8 Results from the optimisation process for down-milling

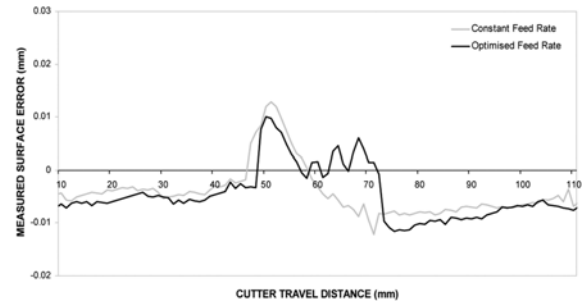


Fig. 9 The measured SE in straight and corner segments of the controlled surfaces with UM

required accuracy achieved. In this case, machining time and inspection time will be wasted but the SE can be corrected successfully. In both types of end-milling (up- and DM) the largest deviation of the cutter is predicted to be at the beginning of the corner where the engagement angle is at its highest value (travel distance = 48 mm).

4. Results and discussion

After generating the new feed-rate data for up- and DM, two test pieces were machined applying the new cutting conditions. The geometry of the part is the same as shown in Fig. 6. The measured SE for UM with constant and variable feed rate is presented in Fig. 9. As The first conclusion from the results is that the SE for the two machined surfaces is well within the tolerance. As predicted, cutting the straight parts of the tool path is more stable, with small variations in SE. In the transient parts, and especially at the corner, the SE varies noticeably. The SE resulting from the variable feed-rate application is larger in the straight segments compared to the error for the corresponding surface machined with constant feed rate. But at the corner, the peak SE obtained from the constant feed-rate cutting is larger than the equivalent error of the surface machined with variable feed-rate conditions. Taking into consideration the larger values of the variable feed rate compared to the constant feed rate it can be concluded that the optimised cutting conditions satisfy the design requirements and create a more efficient milling process. Compared to DM, the radial force F_Y in UM is smaller, when the other process conditions are the same. This creates a smaller SE and a better accuracy in UM. The comparison of the measured SEs with the predicted radial cutting-tool deviations presented in Fig. 7 shows good agreement between them. The SE resulting from the constant cutting condition

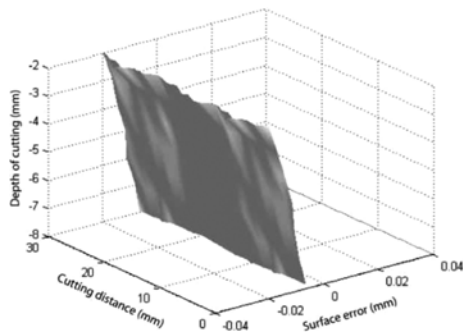


Fig. 10 The measured SE in straight segment as a result of UM

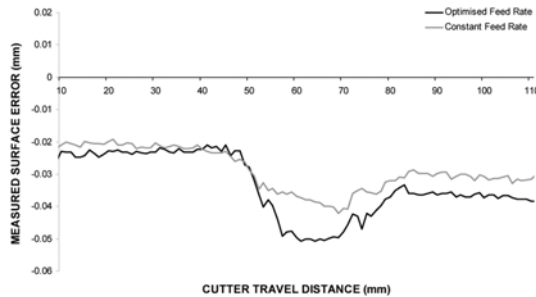


Fig. 11 The measured SE when down-milling was applied

reaches its peak value at the beginning of the corner cutting and then gradually decreases.

The predicted cutting-tool radial deviation follows a similar trend. The variable feed-rate was generated with the aim of keeping the SE and the predicted radial cutting-tool deviation at the highest allowable level. At the corner the predicted radial deviation is constant and analogous results were obtained for the SE. The influence of the different errors during the milling process resulted in variation of the measured SE, but the main trend is evident. The SE results for the straight segments for both constant and variable feed-rate conditions are in good agreement with the predicted radial deviation of the cutting tool. Fig. 10 presents the measured SE in the straight segment of cutting when UM is involved in the milling process. The SE differs from the trend of the predicted cutting-tool deflection shown in Fig. 3. The cutting-tool deflection has small values in the presented case of finishing cutting and does not contribute to the SE significantly. The other errors that are present during the milling predominate over the final SE. In the surface cut with variable feed rate, the largest value of the SE is around the maximum allowable of -0.050 mm. Both SE curves generally follow the trends of the predicted cutter deviation shown in Fig. 8. For the surface cut with constant feed rate, the SE starts to increase after the beginning of the transient segment. The changes in SE values reflect the larger chip thickness at the corner, compared with the straight cutting. In the corner cutting the increase of the SE is not significant, showing a trend of keeping the SE almost constant. During the second transient cut, where the cutting tool is leaving the corner, the SE decreases until the chip thickness becomes constant.

For the surface cut with variable feed rate, the optimised cutting conditions hold the SE at higher values during the corner milling. At the corner, the curve representing the variable cutting condition is in good agreement with the predicted radial cutting-tool deviation (shown in Fig. 8). The measured results prove the ability of the variable feed-

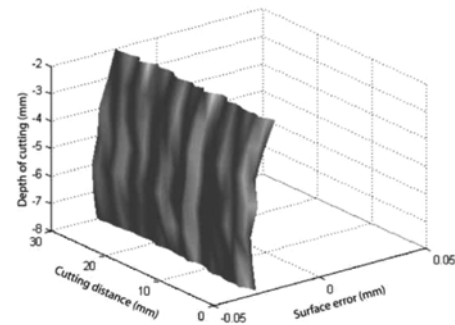


Fig. 12 The measured SE in straight segment as a result of DM

Table 2 Summary of key machining measurements for the optimised and constant feed-rate conditions (magnitude values of the SE are given)

	Up-milling		Down-milling	
	Constant Feed Rate	Optimised Feed Rate	Constant Feed Rate	Optimised Feed Rate
Maximum Measured SE, (mm)	0.0129	0.0115	0.0421	0.0506
Measured Surface Roughness R_a , (μm)	0.0680	0.2620	0.1950	0.2530
Finishing Time (± 1 s) (s)	55.0	12.0	97.0	25.0

rate condition to overcome the increase of the chip thickness in the corner segment.

The second test piece was cut using DM and the SE results from this cutting trial are presented in Fig. 11.

The SE results, when DM was employed, are significantly different than the results for UM. Despite the fact that the feed rates (constant and variable) have lower values in DM, the SE obtained with this type of milling is considerably larger. The measured SE results in a straight segment of the tool path, when DM was engaged are presented in Fig. 12. There is a good agreement between the predicted cutting-tool deflection shown in Fig. 4 and the measured SE.

The results from the test pieces cut with up- and DM are summarised in Table 2. UM demonstrates better results than DM in terms of process efficiency, surface accuracy and surface roughness. The overall SE and predicted cutter radial deviation in UM are lower than the same parameters in DM. At the same time, the feed-rate generated for UM is larger than the feed-rate in DM when the same process requirements have been applied.

The maximum SE in DM is significant due to the specifics of this type of milling. Besides the fact that the radial cutting force in DM is larger than the same force in UM, in DM the F_Y force is directed out of the machined surface and there is nothing to resist the cutter deviation. In UM when the radial force becomes larger its direction is towards the machined surface, which resists deflection. The surface roughness results do not exceed the required surface roughness $R_a = 0.80 \mu\text{m}$, and also establish UM as the better method for finishing milling. The constant feed-rate condition creates lower roughness than the surface roughness of the strips cut with optimised feed-rate conditions. The roughness measurements were taken from the plane parts of the machined surface (Fig. 6 straight segments A and straight segments B), where the variable feed rate is at its highest and the direction is along the tool path. In both types of milling the operations

cut with optimised feed-rate are more efficient than the operations with constant feed rate. For UM, the machining time of the optimised tool path is 78% shorter than the machining time of the operation with constant feed rate. In DM the machining time of the optimised operation is 74% of the machining time with constant feed-rate cutting. This geometry was deliberately designed to create extreme cutting conditions. The experimental results confirm the predicted trend. Comparing the finishing machining times, UM is 46% more efficient than DM. These results contradict the recommendations made by Landon *et al.*⁴ Landon *et al.*⁴ accept that the SE in UM is lower than the same error in DM; but their results show larger values for the surface roughness in UM. They conclude that DM is better for finishing operations than UM because it produces better surface finish, and prevents the cutting tool from rapid wear. All experimental results from this research demonstrate the advantage of UM over DM. Also, they are in agreement with the results of other researchers (Lee and Ko⁶ and Toh.¹¹ The effect of different radial and axial depth of cutting on the surface accuracy needs to be compared when up- and DM are involved. The investigation of the cutting tool wear in up- and DM will contribute to the overall process capability assessment.

The corner-cutting model and geometry employed in this research work cover a variety of realistic cutting conditions, which can be found in a range of end-milling profiles. Previous researchers, such as Loftus and Wang,¹² have investigated simpler cutting scenarios in which the roughed surface is an offset of the finished surface, and the cutting allowance is constant for the whole contour. The model presented here is capable of defining the cutter engagement under various cutting conditions. The experiments presented in this paper confirm the need for a wider use of end-milling optimisation that takes into consideration the work-piece material, the tool-path geometry, the design tolerances and the cutting-tool specification, otherwise worst-case feed-rate settings will predominate.

5. Conclusions

This paper presents the specifics of the two types of end-milling, up- and DM, in the context of process planning of a finishing operation for machining complex pocket features. The chip formation and cutting forces create distinguishable forms of SE when up- and DM are applied. The required surface accuracy has been obtained by applying the optimisation mechanism which adjusts the feed rate to a limiting value. The limiting value is defined by the required surface tolerance and the surface roughness. Two different cutting conditions of each type of end-milling have been simulated and experimentally verified. The advantage of the variable cutting conditions over the constant cutting conditions is significant in both up- and DM processes as presented in Table 2. UM has appeared as the more efficient type of end-milling, compared to DM. The results show that the finishing machining time can be reduced in both machining with constant and with variable feed rate by applying UM. The measured SE and surface roughness have lower values in the work-piece machined with UM than in the test piece cut with DM. At the same time, the feed-rate generated for UM is larger than the feed-rate in DM when the same process requirements have been applied. The predicted and

experimental results confirm the importance of the type of end-milling engaged in finishing cutting when complex pocket type surfaces are machined. The corner cutting was demonstrated as a critical case of finishing cutting, which needs special analysis and planning, regarding the SE and the type of end-milling used for its machining.

REFERENCES

1. Stori, J. A., Wright, P. K., and King, C., "Integration of process simulation in machining parameter optimization," *ASME Journal of Manufacturing Science and Engineering*, Vol. 121, No. 1, pp. 134-143, 1999.
2. Li, Z. Z., Zheng, M., Zheng, L., Wu, Z. J., and Liu, D. C., "A solid model-based milling process simulation and optimization system integrated with CAD/CAM," *Journal of Materials Processing Technology*, Vol. 138, pp. 513-517, 2003.
3. Lee, S. and Lee, J., "Real-time inertia compensation for multi-axis CNC machine tools," *Int. J. Precis. Eng. Manuf.*, Vol. 13, No. 9, pp. 1655-1659, 2012.
4. Landon, Y., Segonds, P., Lascoumes, P., and Lagarrigue, P., "Tool positioning error (TPE) characterisation in milling," *International Journal of Machine Tools and Manufacture*, Vol. 44, pp. 457-464, 2004.
5. Hatna, A., Grieve, R. J., and Broomhead, P., "Automatic CNC milling of pockets: geometric and technological issues," *Computer Integrated Manufacturing Systems*, Vol. 11, pp. 309-330, 1998.
6. Lee, S. K. and Ko, S. L., "Improvement of the accuracy in the machining of a deep shoulder cut by end milling," *Journal of Materials Processing Technology*, Vol. 111, pp. 244-249, 2001.
7. Dotcheva, M. and Millward, H., "The application of tolerance analysis to the theoretical and experimental evaluation of a CNC corner-milling operation," *Journal of Materials Processing Technology*, Vol. 170, pp. 284-297, 2005.
8. Gere, J. and Timoshenko, S., "Mechanics of Materials, 3rd edition," Chapman and Hall, 1995.
9. Xu, A. P., Qu, Y. X., Zhang, D. W., and Huang, T., "Simulation and experimental investigation of the end milling process considering the cutter flexibility," *International Journal of Machine Tools and Manufacture*, Vol. 43, pp. 283-292, 2003.
10. Childs, T. H. C., Maekawa, K., Obikawa, T., and Yamane, Y., "Metal Machining-Theory and Application," London: Arnold, 2000.
11. Toh, C. K., "Surface topography analysis when high-speed rough milling hardened steel," *Materials and Manufacturing Processes*, Vol. 18, No. 6, pp. 849-862, 2003.
12. Loftus, M. and Wang, D., "A theory to support the high-speed computer numerical control machining of corner profiles," *Proceedings of IMechE Part B: Journal of Engineering Manufacture*, Vol. 216, pp. 643-647, 2002.